

## Supporting Information

### Amorphous Silk Nanofiber Solutions for Fabricating Silk-Based Functional Materials

*Xiaodan Dong<sup>a,b</sup>, Qun Zhao<sup>a,b</sup>, Liying Xiao<sup>a,b</sup>, Qiang Lu<sup>a,b,\*</sup>, and David L Kaplan<sup>c</sup>*

<sup>a</sup>Collaborative Innovation Center of Suzhou Nano Science and Technology, Soochow  
University, Suzhou 215123, People's Republic of China

<sup>b</sup>National Engineering Laboratory for Modern Silk, Soochow University, Suzhou  
215123, People's Republic of China

<sup>c</sup>Department of Biomedical Engineering, Tufts University, Medford, MA 02155, USA

## **Experimental Section**

### **Dynamic light scattering (DLS)**

Dynamic light scattering (DLS) measurement was performed with a Zetasizer (Nano ZS, Malvern, Worcestershire, UK) using an angle of  $173^\circ$  and equipped with a 633-nm He–Ne laser. 1ml of silk solution was used in disposable polystyrene cuvettes with a 10-mm path length. All data were collected at 25 °C.

### **Zeta Potential**

Zeta potentials of silk solutions were recorded by zeta potential measurement. For the measurement, one milliliter of the solution was loaded to a Zetasizer (Nano ZS, Malvern, Worcestershire, UK) at 25 °C.

### **Atomic Force Microscopy (AFM)**

For AFM experiments, SF-FA were diluted to below 0.001 wt% to avoid masking the original morphology by multilayers of silk.<sup>1</sup> A total of 2  $\mu\text{L}$  of the diluted solution was dropped onto freshly cleaved  $4 \times 4 \text{ mm}^2$  mica surfaces and spin coating. The morphology of silk fibroin was observed by AFM (Nanoscope V, Veeco, NY, USA) in air. A 225  $\mu\text{m}$  long silicon cantilever with a spring constant of  $3 \text{ N m}^{-1}$  was used in tapping mode at 0.5-1 Hz scan rate.

### **SEM**

The morphology of samples was observed using scanning electron microscopy (SEM, S-4800, Hitachi, Tokyo, Japan) at 3kV. For the solution samples, the samples were diluted to below 0.001 wt% to avoid masking the original morphology, 2  $\mu\text{L}$  of samples was added directly on top of a conductive tape mounted on a SEM sample

stub and dried in air. As for scaffolds and films, the samples were fractured in liquid nitrogen. Before SEM examination, all samples were coated with platinum for 60s.

### **Circular dichroism (CD)**

The secondary structures of the silk solutions were collected using a Jasco-815 CD spectrophotometer (Jasco Co., Japan).<sup>2</sup> CD spectra were recorded from 250 to 190 nm wavelengths at a scanning rate of 100 nm min<sup>-1</sup> with an accumulation of five scans at 25 °C. The results were averaged from three repeated experiments.

### **FTIR**

FTIR was conducted on a Nicolet FTIR 5700 spectrometer (Thermo Scientific, FL, USA) equipped with a MIRacle<sup>TM</sup> attenuated total reflection (ATR) Ge crystal cell in reflection mode.<sup>3,4</sup> For each measurement, 64 scans were coded with a resolution of 4 cm<sup>-1</sup>, with the wavenumber ranging from 400 to 4000 cm<sup>-1</sup>.

### **Raman Spectra**

The secondary structures of the silk solutions were measured with a Raman spectrometer (Renishaw, 633 nm diode laser with a resolution of 2 cm<sup>-1</sup>, exposure time 10s and laser power 100%) based on the freeze-dried samples.<sup>5</sup> The samples were placed at -20 °C for about 12 h, and then lyophilized for about 48 h to achieve freeze-dried samples.

### **DSC**

Samples of about 5mg were encapsulated in aluminum pans and heated in a TA Instrument Q2000 DSC (TA Instruments, New Castle, DE, USA) with a dry nitrogen gas flow of 50 ml·min<sup>-1</sup>. The instrument was calibrated for empty cell baseline and

with indium for heat flow and temperature before the test. Temperature-modulated differential scanning calorimetry (TMDSC) measurements were performed using a TA instrument Q2000, equipped with a refrigerated cooling system.<sup>4</sup> The samples were heated from -30 to 350°C at 2°C min<sup>-1</sup> with temperature modulation amplitudes of 0.318°C and a modulation period of 60s.

### **Dynamic oscillatory rheology**

Rheological studies were run on a Rheometer (AR2000, TA Instruments, New Castle, USA). Prior to each experimental day, the rheometer underwent a torque map with a 10 Pa s calibration oil. The shear rate was linearly increased from 0.01 to 5000 s<sup>-1</sup> at 25 °C (Ti, 40/2°).<sup>6</sup> Frequency sweeps were collected continuously over a wide frequency range from 1 to 100 rad s<sup>-1</sup> at 25 °C (Ti, 20/1°).<sup>7</sup> All samples were stabilized for 20 min before the measurement.

## Results

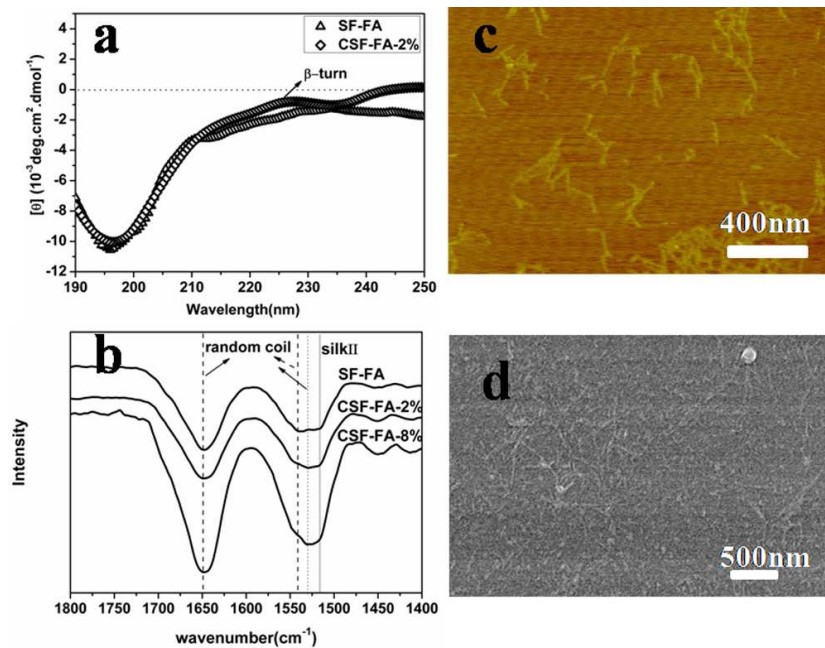


**Figure S1.** Conformations and microstructures of silk in the concentrated process: (a) CD; (b) FTIR of silk fibrion solutions. (c) AFM and (d) SEM of 2wt% silk nanofiber solutions. The samples are as follows: SF-FA, fresh amorphous silk nanofiber solution prepared through the present LiBr-formic solvent; CSF-FA-2%, fresh amorphous silk nanofiber solution were concentrated to 2wt%; CSF-FA-8%, fresh amorphous silk nanofiber solution were concentrated to 8wt%. No significant secondary structure and microstructure changes appeared after concentration.

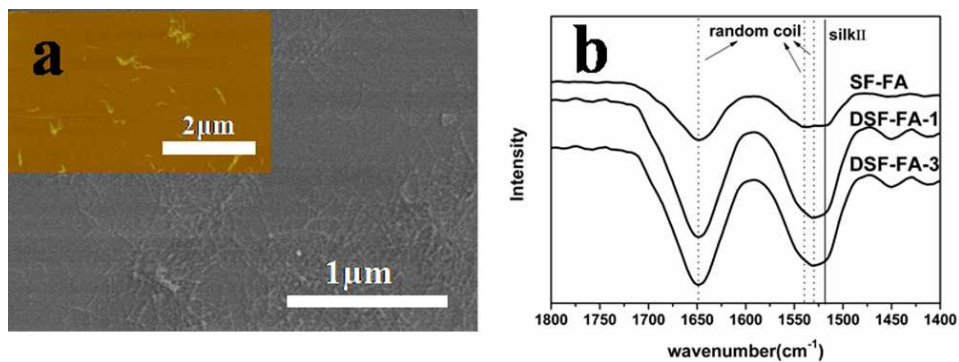


**Figure S2.**(a) SEM, AFM and (b) FTIR of re-dissolved silk nanofiber solutions. The samples are as follows: SF-FA, fresh amorphous silk nanofiber solution prepared through the present LiBr-formic solvent; DSF-FA-1, re-dissolved after silk nanofiber solutions had been freeze-dried, stored at room temperature for one month; DSF-FA-3, re-dissolved after silk nanofiber solutions had been freeze-dried, stored at room temperature for three months.

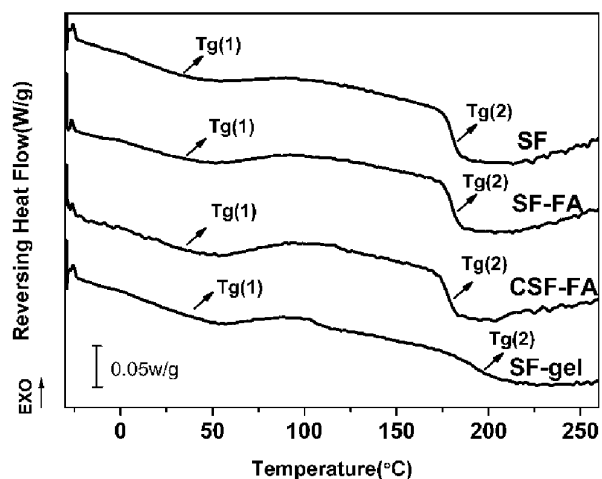


**Figure S3.** Temperature-modulated DSC scans (TMDSC) of different silk solutions.

The samples are as follows: SF-FA, amorphous silk nanofiber solution prepared through the present LiBr-formic solvent; SF, amorphous silk solution prepared through the regular LiBr solvent reported previous; SF-gel, silk nanofibers with high beta-sheet content prepared through a slow concentration–dilution process; CSF-FA, fresh amorphous silk nanofiber solution were concentrated to 8%.

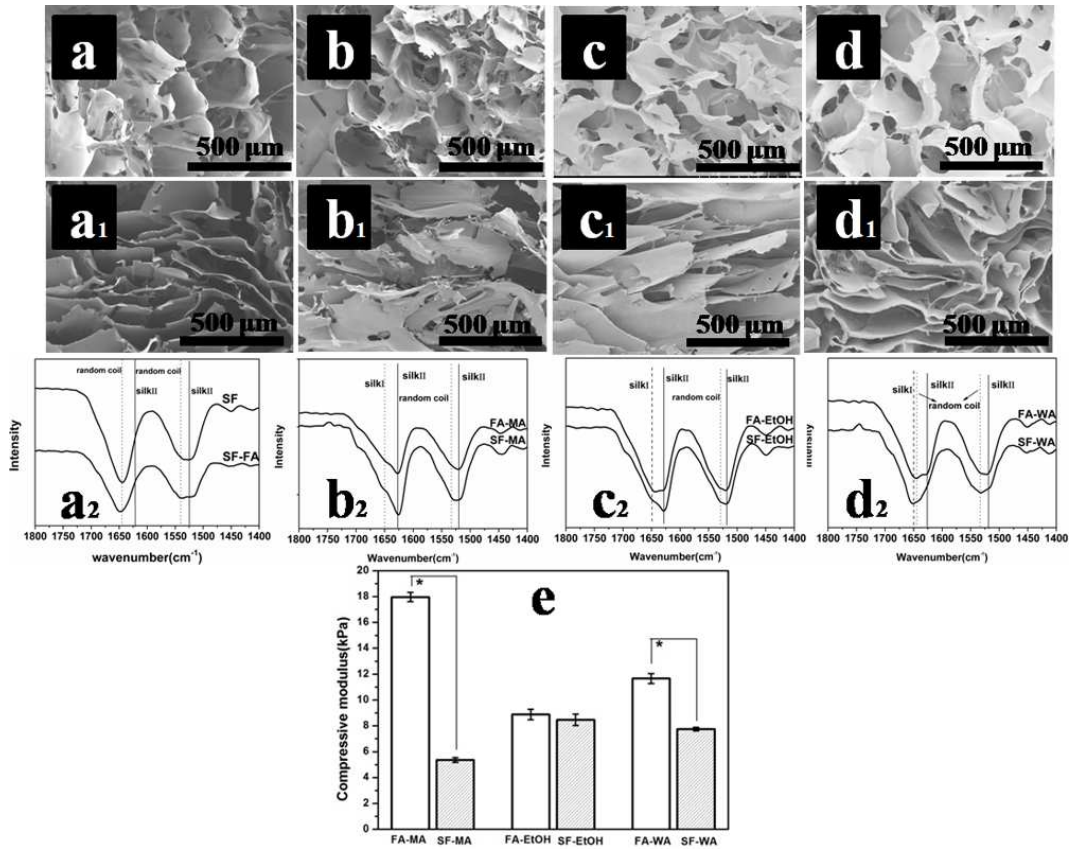


**Figure S4.** The properties of silk scaffolds derived from SF-FA and SF solutions: (a)-(d) SEM images of untreated methanol treated, ethanol treated and water annealing scaffolds derived from SF-FA, respectively; (a<sub>1</sub>-d<sub>1</sub>) SEM images of untreated, methanol treated, ethanol treated and water annealing scaffolds derived from SF, respectively; (a<sub>2</sub>-d<sub>2</sub>) The FTIR spectra of untreated methanol treated, ethanol treated, and water annealing scaffolds derived from SF-FA and SF solutions, respectively; (e) The mechanical properties of the scaffolds derived from SF-FA and SF, respectively. The methanol, ethanol and water annealing scaffolds were termed FA-MA, SF-MA, FA-EtOH, SF-EtOH, FA-WA, SF-WA, respectively. Error bars represent B mean ± standard deviation with N= 5 (\*p < 0.05).



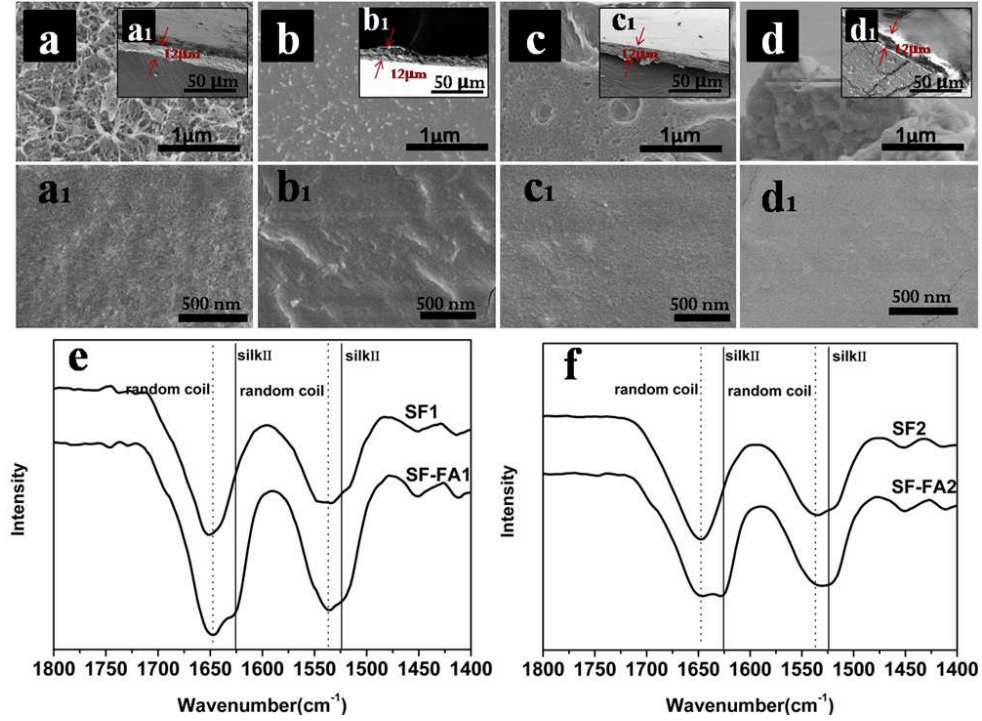


**Figure S5.** The properties of silk films derived from SF-FA and SF solutions: (a)-(d) Cross-section; (a<sub>1</sub>)-(d<sub>1</sub>) surface images; (a<sub>2</sub>)-(d<sub>2</sub>) thickness of films; (e) FTIR of films prepared by 2% silk solutions at room temperature. (f) FTIR of films prepared by 2% silk solutions at 60 °C. (a, a<sub>1</sub> and a<sub>2</sub>) Drying the nanofiber solution overnight at room temperature in fume hood without lid; (b, b<sub>1</sub> and b<sub>2</sub>) Drying the nanoparticle solution overnight at room temperature in fume hood without lid; (c, c<sub>1</sub>, and c<sub>2</sub>) Drying the nanofiber solution overnight at 60 °C in fume hood without lid; (d, d<sub>1</sub> and d<sub>2</sub>) Drying the nanoparticle solution overnight at 60 °C in fume hood without lid.

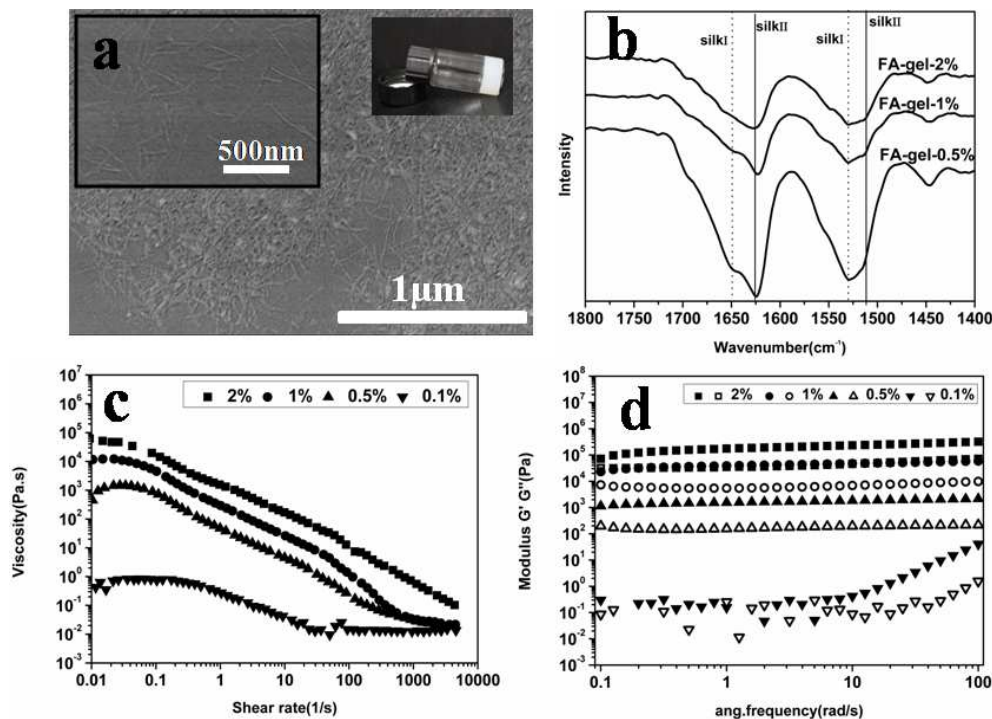


**Figure S6.** Silk hydrogels derived from the amorphous silk nanofibers by treating the solution at 60 °C for about 4 hours: (a) SEM images of the diluted silk hydrogels; (b) FTIR of the hydrogels derived from silk nanofiber solution with various concentrations; (c) Storage modulus ( $G'$ , solid symbols) and loss modulus ( $G''$ , open symbols) versus frequency of the hydrogels with various concentrations. Compared to the previously reported SF-gel, SF-FA also formed hydrogels which were composed of nanofibers and have high crystallinity. The samples are as follows: FA-gel-2%, hydrogels from 2% amorphous silk nanofiber solutions placed at 60 °C for about 4 hours; FA-gel-1%, hydrogels from 1% amorphous silk nanofiber solutions placed at 60 °C for about 4 hours; FA-gel-0.5%, hydrogels from 0.5% amorphous silk nanofiber solutions placed at 60 °C for about 4 hours.

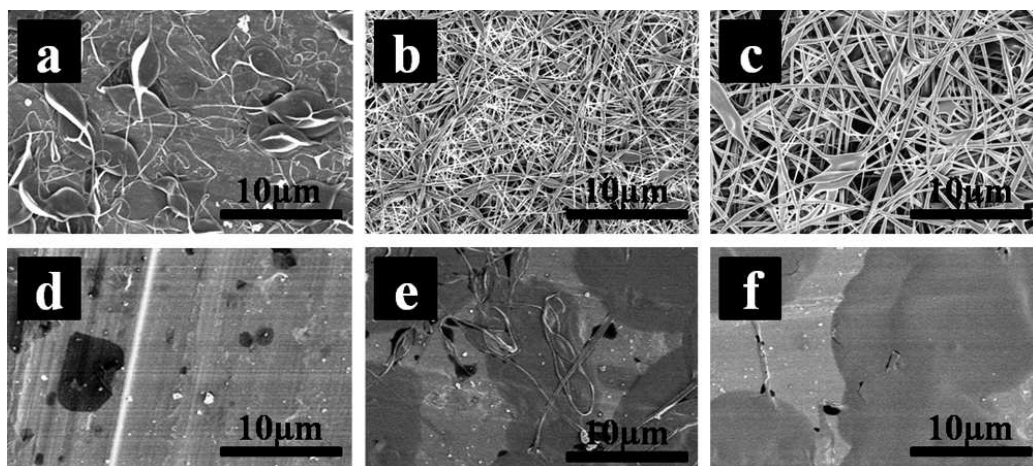


**Figure S7.** The morphology of electrospun silk nanofibers derived from SF-FA and SF solutions: (a)-(c) The SEM images of electorspun silk nanofibers from 2%, 6%, 8% SF-FA and (d)-(f) The failure to form electrospun silk nanofiber from 2%, 6%, 8% SF solution. The samples are as follows: Left, electorspun silk nanofibers from 2% silk solution; Middle, electorspun silk nanofibers from 6% silk solutions; Right, electorspun silk nanofibers from 8% silk solutions.

**Table S1.** Sample abbreviations of SF samples obtained under different conditions

Sample code	preparation method
SF-FA	amorphous silk nanofiber solution prepared through the present LiBr-formic solvent
SF	amorphous silk solution prepared through 9.3M LiBr solvent
SF-gel	silk nanofibers with high beta-sheet content prepared through a slow concentration–dilution process
CSF-FA	fresh amorphous silk nanofiber solution were concentrated to 8%
HSF-FA	silk hydrogels formed by SF-FA
HSF	silk hydrogels formed by SF

**Table S2.** Mechanical properties of silk films prepared by SF and SF-FA. n = 3, average  $\pm$  standard deviation.

Silk Film	Tensile Strength (Mpa)	Elongation at Break (%)
SF-FA1	24.8 $\pm$ 10.8	3.0 $\pm$ 0.5
SF1	26.1 $\pm$ 4.9	7.1 $\pm$ 4.2
SF-FA2	29.1 $\pm$ 13.5	3.8 $\pm$ 0.5
SF2	26.6 $\pm$ 5.5	6.8 $\pm$ 5.1

## Supporting Information References

- (1) Yao, D. Y.; Dong, S.; Lu, Q.; Hu, X.; Kaplan, D. L.; Zhang, B. B.; Zhu, H. S. *Biomacromolecules* **2012**, *13*, 3723-3729.
- (2) Bai, S.; Liu, S.; Zhang, C.; Xu, W.; Lu, Q.; Han, H.; Kaplan, D. L.; Zhu, H. *Acta Biomater.* **2013**, *9*, 7806-7813.
- (3) Lu, Q.; Zhang, X. H.; Hu, X.; Kaplan, D. L. *Macromol. Biosci.* **2010**, *10*, 289-298.
- (4) Lu, Q.; Hu, X.; Wang, X. Q.; Kluge, J. A.; Lu, S. Z.; Cebe, P.; Kaplan, D. L. *Acta Biomater.* **2010**, *6*, 1380-1387.
- (5) Pan, H.; Zhang, Y. P.; Hang, Y. C.; Shao, H. L.; Hu, X. C.; Xu, Y. M.; Feng, C. *Biomacromolecules* **2012**, *13*, 2859-2867.
- (6) Holland, C.; Terry, A. E.; Porter, D.; Vollrath, F. *Polymer*, **2007**, *48*, 3388-3392.
- (7) Leisk, G. G.; Lo, T. J.; Yucel, T.; Lu, Q.; Kaplan, D. L. *Adv. Mater.* **2010**, *22*, 711-715.